Ab initio calculation of the CdSe/CdTe heterojunction band offset using the local-density approximation-1/2 technique with spin-orbit corrections

M. Ribeiro, Jr.,[1,a)] L. R. C. Fonseca,[2] T. Sadowski,[3] and R. Ramprasad[3]
[1]*Centro de Pesquisas Avançadas Wernher von Braun, Av. Alice de Castro P. N. Mattosinho 301, Campinas 13098-392, SP, Brazil*
[2]*Center for Semiconductor Components, State University of Campinas, R. Pandia Calógeras 90, Campinas 13083-870, SP, Brazil*
[3]*Department of Chemical, Materials and Biomolecular Engineering, Institute of Materials Science, University of Connecticut, 97 North Eagleville Road, Storrs, Connecticut 06269, USA*

(Received 24 January 2012; accepted 27 February 2012; published online 6 April 2012)

We performed *ab initio* calculations of the electronic structures of bulk CdSe and CdTe and of their interface. We employed the local-density approximation-1/2 self-energy correction scheme [L. G. Ferreira, M. Marques, and L. K. Teles, Phys. Rev. B **78,** 125116 (2008)] to obtain improved band gaps and band offsets, as well as spin-orbit coupling to further correct the valence band edges. Our results are in good agreement with experimental values for bulk band gaps and reproduce the staggered band alignment characteristic of this system. We found that the spin-orbit effect is of considerable importance for the bulk band gaps, but has little impact on the band offset of this particular system. Moreover, the electronic structure calculated along the 61.4 Å transition region across the CdSe/CdTe interface shows a non-monotonic variation of the bandgap in the range 0.8-1.8 eV. This finding may have important implications to the absorption of light along the interface between these two materials in photovoltaic applications. © *2012 American Institute of Physics*. [http://dx.doi.org/10.1063/1.3699054]

I. INTRODUCTION

Interfaces between dissimilar materials are pervasive in many practical situations. In electronics and optical applications, the electronic structure of the individual materials (e.g., the bandgap) and its variation across the interfaces (e.g., the band offsets) critically determine the device properties. Despite decades of effort, reliable and efficient prediction of band gaps and band off-sets using first principles computations has remained a challenge. Conventional (semi)local electronic exchange-correlation functionals lead to significant underestimation of the band gaps of insulators and, consequently, to uncertainties in the computed band offsets at interfaces.[1] Recent advances to overcome such challenges include the local-density approximation (LDA)-1/2 self-energy correction scheme,[2] the utilization of hybrid exchange-correlation functionals,[3] and the many-body techniques, such as the GW method.[4]

In the present work, we use the LDA-1/2 method to determine the electronic structure of CdTe, CdSe, and the CdTe-CdSe heterostructure. The large system sizes necessitated by the CdTe/CdSe precludes the usage of the GW method, while the intrinsic difficulty to determine a common mixing parameter for the two different materials forming the interface makes hybrid functionals less attractive. Moreover, the LDA-1/2 method has proven itself successful in predicting accurate band gaps[2] for a large number of semiconductors and insulators, as well as band offsets for the Si/SiO_2 (Ref. 5) and GaAs/AlGaAs (Ref. 6) interfaces, at a computational cost similar to regular discrete Fourier transform (DFT)/LDA.

The choice of the CdTe and CdSe systems is motivated by their already widespread use in current second generation thin film solar cells[7] and their potential use in third generation nanocrystal- or nanowire-based photo-voltaic architectures.[8] The attractiveness of these materials arises from their bandgap value, which falls within the solar spectrum, thereby enabling the efficient creation of electron-hole pairs (or excitons) by solar photons. Nevertheless, a major factor that controls the efficiency of photovoltaic systems is the efficient dissociation of photo- generated excitons. Exciton dissociation in nanocrystal- or nanowire-based architectures may be accomplished by suitable interfaces between dissimilar materials, e.g., the CdTe-CdSe interface, which displays a Type II (or staggered) band offset.[9]

The intent of the present work is thus a first-ever reliable prediction of the electronic structure of bulk CdTe, bulk CdSe, and the CdTe-CdSe heterostructure. We find that the band gaps are significantly affected by spin-orbit effects and are well-predicted (with respect to experiments) by the LDA-1/2 treatment. The band offsets are affected by strain, and there are gradual band edges transitions across the interface over a distance of 61 Å (with a concomitant variation of the bandgap in the 0.8-1.8 eV range in this transition region).

This paper is organized as follows: In Sec. II, we describe the computational methods employed, including a brief description of the LDA-1/2 scheme, and the atomic model for the bulk materials and their interface. In Sec. III, we describe our calculated band gaps for the bulk systems and band offsets for the interfaces with and without the self-

[a)]Electronic mail: maurofsrj@gmail.com. Also at Departamento de Física dos Materiais e Mecânica, Instituto de Física, Universidade de São Paulo, São Paulo 05315-970, SP, Brazil.

TABLE I. Bulk and strained LDA lattice parameters for wz-CdSe and wz-CdTe. *str* LDA values refer to CdTe (CdSe) strained to the CdSe (CdTe) *c* and *a* lattice parameters. Experimental values taken from Ref. 17.

Lattice parameters (Å)						
	CdTe			CdSe		
	LDA	*str* LDA	Expt.	LDA	*str* LDA	Expt.
a	4.52	4.64	4.58	4.24	4.19	4.30
c	7.42	6.95	7.50	6.95	7.42	7.02

energy correction and spin-orbit coupling. Finally, we draw our conclusions in Sec. IV.

II. METHODS AND INTERFACE MODELS

Our total-energy and electronic structure calculations were based on the density functional theory (DFT) within the local density approximation (LDA).[10] For the description of the interactions among electrons and nuclei, we used the frozen-core projector augmented-wave,[11] as implemented in the VASP code.[12] The cutoff for the plane wave expansion of the wavefunctions was 274 eV. The *k*-space integrals were approximated by sums over a special mesh of the Monkhorst-Pack type[13] in the irreducible part of the Brillouin zone. For bulk and slab calculations, we used $9 \times 9 \times 9$ and $9 \times 9 \times 1$ *k*-meshes respectively, both including the Γ point, and a denser $12 \times 12 \times 1$ mesh for the density of states calculations. To account for the band splittings at the valence band maximum (VBM) of each bulk material, we included spin-orbit (SO) coupling explicitly in the calculations, thus making the energy dependent on the direction of the magnetic moment. As shown below, the SO splitting is of considerable importance to the reproduction of experimental band gaps. SO was introduced in our slab calculations *a posteriori* as rigid shifts of the valence band edges (VBE) with values given by the calculated bulk band splittings.

Throughout this work, CdSe and CdTe are assumed to be in the wurtzite phase. Our calculated bulk lattice constants, shown in Table I, are within 1.5% and 1.4% (1.5% and 1.6%) of the experimental values for the *a* (*c*) lattice constants of CdTe and CdSe, respectively, which is typical of well-converged LDA calculations. The CdSe- CdTe heterostructure supercell was built with its interface parallel to the a-c plane. The $a_{||}$ (parallel to the interface) and *c* lattice parameters of the CdTe (CdSe) slab were fit to the CdSe (CdTe) slab values, while the normal lattice parameter $a_{\perp}$ was relaxed, partially relieving the strain energy. This setup was motivated by applications of these systems in multijunction solar cells and in core/shell (0001) CdSe/CdTe nanowires under strain, as described in Ref. 9. Since it is well known that the electronic structure of semiconductors is sensitive to strain,[14] two different strain situations were considered. Under one situation, referred to as hetero@CdSe, the lattice parameters along the plane parallel to the interface were constrained to be at the equilibrium CdSe values, while in the other, referred to as hetero@CdTe, these lattice parameters were fixed at the corresponding CdTe values. For thin enough films, lattice-mismatched heterostructures can be grown without misfit defects, as first studied by Matthews and Blakeslee.[15] Because the strain for our interfaces is about 6.4%, the defect-free approximation is only realistic for films a few atomic layers thick,[16] which is the case in this study.

To improve on the LDA underestimation of band gaps, we employed the LDA-1/2 method,[2] which has previously shown excellent results for band gaps[2] and band offsets.[5,6] The LDA-1/2 method aims at removing the spurious electrostatic electron self-energy in the band structure calculations of crystals. It follows from Slater's transition state technique,[18,19] which yields excellent results for the ionization potentials of atoms. To extend this idea to crystals, in LDA-1/2, one adds to the crystalline potential an atomic "self-energy potential", defined as the difference between the Kohn-Sham atomic potential and the potential of a system lacking half electronic charge (–1/2 e). In ionic insulators and semiconductors, only the anionic self-energy potential is important, because the valence band, composed mostly of anion states, is more localized than the conduction band and therefore is more disrupted by its larger self-energy. In the present study, only modifying the Se and Te *p*-orbitals proved necessary. Because the self-energy is local, its long-range Coulomb potential tail needs to be bounded by a cutoff radius (CUT) to avoid overlapping with the self-energy potentials of the other anions in the lattice. This procedure follows a variational principle without adjustable parameters. In addition to accuracy, this technique has almost the same computational cost as usual LDA.

Figure 1 shows the optimization of the CUT parameter for Se and Te. The optimal CUT values are found at the maximum of the bulk band gaps, with values 3.7 and 4.0 a.u.s (a.u.) for the Se and Te *p*-orbitals, respectively. All LDA-1/2 calculations were performed with LDA-relaxed lattice parameters (see Table I).

III. RESULTS

A. Bulk systems at equilibrium and under strain

Figure 2 shows the CdTe and CdSe band structures obtained with LDA and LDA-1/2. Without SO correction, the calculated wurtzite CdTe direct bandgap is 1.78 eV,

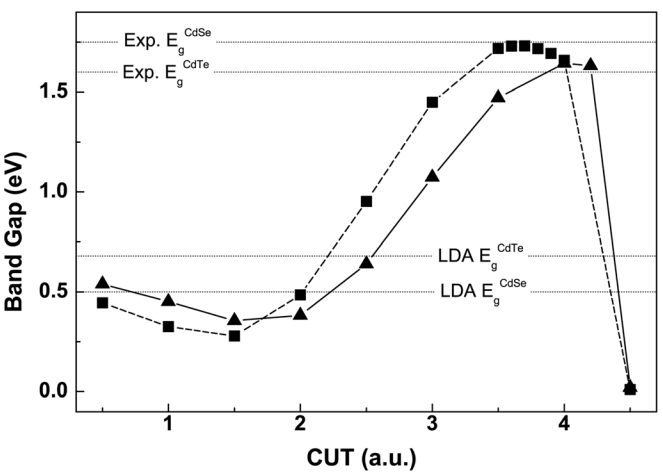

FIG. 1. Variational determination of the CUT parameter for the anions. Spin-orbit coupling not included.

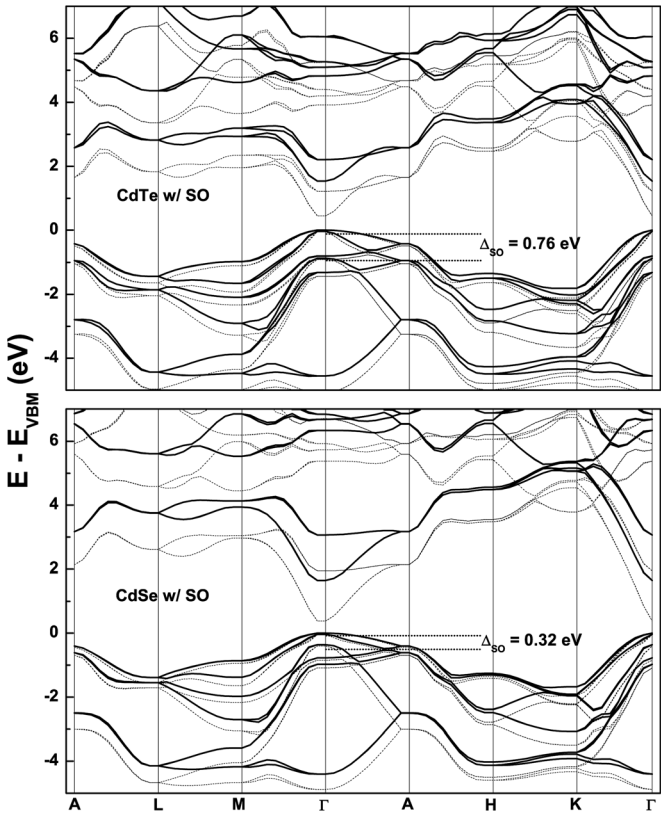

FIG. 2. LDA-1/2 (solid) and LDA (dotted) band structures for bulk wurtzite CdTe (top) and CdSe (bottom), both including SO coupling. Self-energy correction changes very little the LDA SO energies, but have a considerable impact on the LDA band gaps. Reference energy taken at the top of the valence bands.

consistent with previous GW calculations.[20] SO effects reduce the bandgap by 0.23 eV to 1.55 eV, in good agreement with the experimental value of 1.60 eV for wurtzite CdTe.[21] Unlike zinc blende CdTe, where the values we obtained for the band splitting parameter Δ_{SO} employing either LDA and LDA-1/2 pseudopotentials are quite close (0.87 and 0.85 eV, respectively, in good agreement with experimental values 0.90–0.95 eV[17,22,23]), for wurtzite CdTe, we found a larger difference, 0.85 and 0.76 eV obtained with LDA and LDA-1/2, respectively. We have been unable to find experimental values for wurtzite CdTe to compare with. Our calculated direct bandgap of wurtzite CdSe without SO coupling is 1.77 eV, in good agreement with the experimental bandgap of 1.75 eV. The inclusion of SO coupling reduces the CdSe bandgap to 1.66 eV, a decrease of only 0.11 eV, about half the decrease obtained for CdTe. SO correction to the CdSe band structure was also included by other authors employing semiempirical methods,[24–26] DFT,[27] and GW.[20] Our LDA and LDA- 1/2 values of Δ_{SO} for wurtzite-CdSe are quite similar, 0.36 eV and 0.32 eV, respectively, while the experimental results vary in the range 0.39–0.41 eV.[17,28,29]

Table II summarizes the effects of LDA-1/2 and SO energy corrections on the bulk band gaps of bulk wz-CdTe and wz-CdSe. Notice that Δ_{SO} is about twice the LDA bandgap energy, E_g(SO), for CdTe and close to the value of E_g(SO) for CdSe. The table also shows the value of the bandgaps under

TABLE II. Bulk wurtzite CdSe and CdTe band gap energies without [E_g] and with [E_g(SO)] spin-orbit coupling. Also shown are the band splitting parameters, Δ_{SO}. For comparison, band gap energies for strained structures, including spin-orbit [$E_g^{blk\ str}$(SO)] were obtained from bulk LDA-1/2 calculations of CdSe (CdTe) strained to the CdTe (CdSe) lattice parameters c and $a_{||}$ and $a_{\perp}$ relaxed to its equilibrium value. Without strain, $a_{||} = a_{\perp}$. Experimental values are shown for comparison.[17]

Bulk band gaps (eV)						
	CdTe			CdSe		
	LDA	LDA-1/2	Expt.	LDA	LDA-1/2	Expt.
E_g	0.68	1.78		0.50	1.77	
E_g (SO)	0.45	1.55	1.60	0.38	1.66	1.75
$E_g^{blk\ str}$(SO)		1.62			1.28	
Δ_{SO}	0.85	0.76	0.95[a]	0.36	0.32	0.39–0.41

[a]Measured at 300 K.[17]

biaxial strain, where the $a_{||}$ and c lattice parameters of the CdTe (CdSe) bulk were fit to the CdSe (CdTe) bulk values (~6% lattice mismatch), while the $a_{\perp}$ lattice parameter was relaxed, releasing some of the strain energy. Under strain, the band structures undergo considerable changes, as shown in Fig. 3. With LDA, the strained CdSe bandgap is found to be indirect. On the other hand, with LDA-1/2, strained CdSe displays a direct bandgap, as in the unstrained case. The CdSe and CdTe bulk-strained band gaps (including SO) are 1.28 eV and 1.62 eV, respectively. Moreover, under compressive (in the case of CdTe) and tensile (in the case of CdSe) strain, the bandgap of CdTe (CdSe) increases (decreases) as expected.

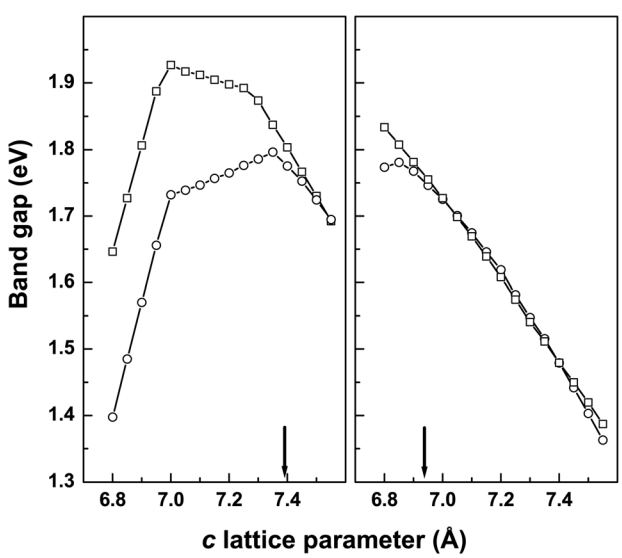

FIG. 3. Bulk band gaps (without SO) versus c lattice parameter for CdTe (left) and CdSe (right). We have considered two cases: squares (case A) representing calculations in which we simply fixed the a lattice parameter to the bulk LDA-calculated value; circles (case B) representing calculations in which we firstly found the optimized LDA-calculated a lattice parameter corresponding to each strained c. Vertical arrows indicate the LDA equilibrium c (which we label c_0). We label an equilibrium c lattice parameter as c_0 (indicated as vertical arrows in figure), which may be associated to CdTe or CdSe. Notice the strange behavior near the equilibrium for CdTe, which presents a turning point close to c_0, while for CdSe, the slope is almost constant in the range, except around c_0 in case B.

B. Heterostructures: Hetero@CdTe and hetero@CdSe

Two heterostructure configurations were considered. In the first, CdTe acts as the substrate and CdSe is lattice matched to it (hetero@CdTe). In the second, the system is inverted, i.e., CdSe is considered as the substrate and CdTe is lattice-matched to it (hetero@CdSe). In both cases, the atomic positions are relaxed to get a more precise charge density distribution at the interface. To guarantee that the interfaces are far enough to avoid interactions and charge confinement, 32 atomic planes of each material were included in the model. This number of planes was the minimum necessary to obtain well-converged band offsets from the density of states projected on the atomic planes (PDOS), which is useful to investigate the band edges along the transition region between the two materials. Table III shows that, for these many planes, quantum confinement is minimized, resulting in heterostructure band gaps (obtained as far as possible from the interfaces), in good agreement with their corresponding bulk values. The difference between bulk and heterostructure band gaps is never larger than 0.13 eV, indicating good convergence.

The band offsets were calculated using the partial density of states (PDOS) projected onto atomic planes, as similarly done earlier.[30,31] Figure 4 shows the LDA and LDA-1/2 PDOS for each of the 64 atomic planes (32 planes for each material) along the CdSe/CdTe supercell for the case hetero@CdSe (the case hetero@CdTe is similar and is not shown here). The corresponding atomic planes and interfaces are also shown. Away from the interfaces, toward the middle of each film (CdTe in the bottom, CdSe on the top), we see the convergence of the CB and VB edges, as well as of the band gaps, to their bulk values. Figure 4 also reveals the difficulty of properly finding the edges of the staggered band offset using LDA. Indeed, the top figure shows that CdTe conduction states are very close to CdSe top valence band, resulting in a bandgap of only 0.15 eV for the heterostructure. Because LDA-1/2 opens up the band gaps at each side of the interface, resulting in a heterostructure bandgap of 0.83 eV, the band edges are more easily identified in this case.

Figure 5 shows the variation of the LDA-1/2 band gaps and band offsets along the heterostructure, starting from the CdTe side (left), crossing the interface, and finishing at the CdSe side (right) for the two configurations (hetero@CdTe and hetero@CdSe). SO effects investigated in the bulk calculations are not included here, due to the extra computational demand. Due to the staggered band alignment, the heterostructure conduction (valence) band edge (CBE (VBE)) is composed of CdSe (CdTe) wave functions. Notice that the VBE transition from the CdSe to CdTe character is somewhat faster than the CBE transition in the opposite direction. Moreover, the CBE transition occurs entirely in the CdTe side of the interface, while the VBE transition occurs entirely in the CdSe side, independently of the choice of configuration (hetero@CdTe or hetero@CdSe), revealing the greater localization of the valence (conduction) band edges along the interface at the CdTe (CdSe) side. Figure 5 also shows that the electronic transition region spans 24 atomic planes, or ≈61.4 Å, and is nearly centred at the physical interface. These two features are independent of the choice of configuration. Because the transition regions for the CBE and VBE span several atomic planes, the bandgap along the transition region varies non-monotonically, ranging from ≈0.76 (0.82) eV near the interface to 1.64 (1.27) eV in the CdSe side and 1.82 (1.78) eV in the CdTe side for hetero@CdSe (hetero@CdTe). Such behavior should be common to staggered band alignments whenever the length of the transition region is non-zero. This is quite different from non-staggered band alignments, such as the Si/SiO_2 (Ref. 5) and GaAs/AlAs (Ref. 6) interfaces, where the bandgap varies monotonically in the transition region. The ≈0.8-1.8 eV bandgap variation

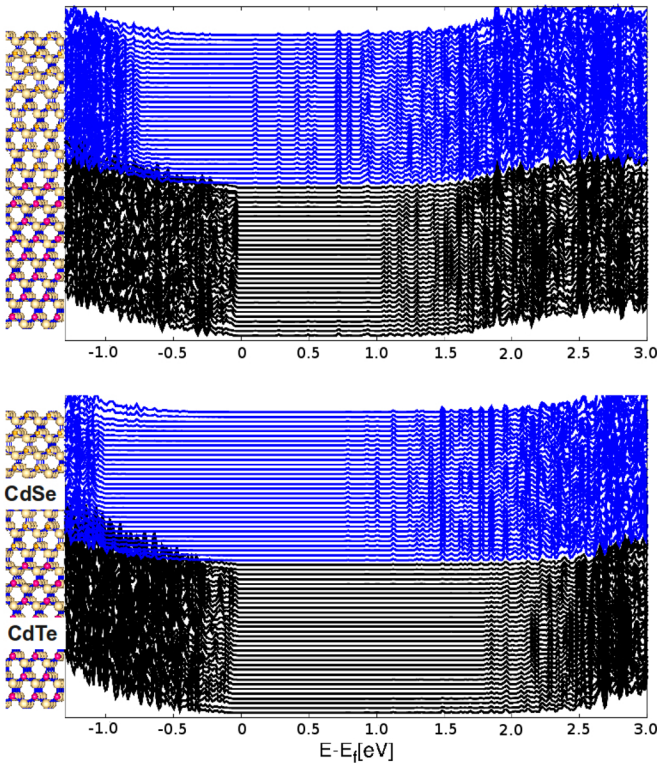

FIG. 4. Plane-by-plane CdSe/CdTe projected density of states (PDOS) for hetero@CdSe (for hetero@CdTe, the results are similar). Calculations based on LDA (top) and LDA-1/2 (bottom). The PDOS lines have been spaced for clarity by approximately the same amount as the atomic plane spacing indicated by the heterostructure models on the left, where only the first atomic planes away from the interface are shown.

TABLE III. Strained CdSe and CdTe bulk and heterostructure LDA-1/2 band gaps. *blk str* values refer to bulk CdTe (CdSe) strained to the CdSe (CdTe) c and $a_{||}$ lattice parameters, with $a_{\perp}$ relaxed to its equilibrium value. Without strain, $a_{||} = a_{\perp}$. *het* is similar to *blk str*, except that the band gaps were obtained from heterostructure calculations.

	Heterostructure band gaps (eV)			
	CdTe lattice parameters		CdSe lattice parameters	
$E_g^{blk\ str}$	CdSe:	1.35	CdSe:	1.77
	CdTe:	1.78	CdTe:	1.87
E_g^{het}	CdSe:	1.27	CdSe:	1.64
	CdTe:	1.78	CdTe:	1.82

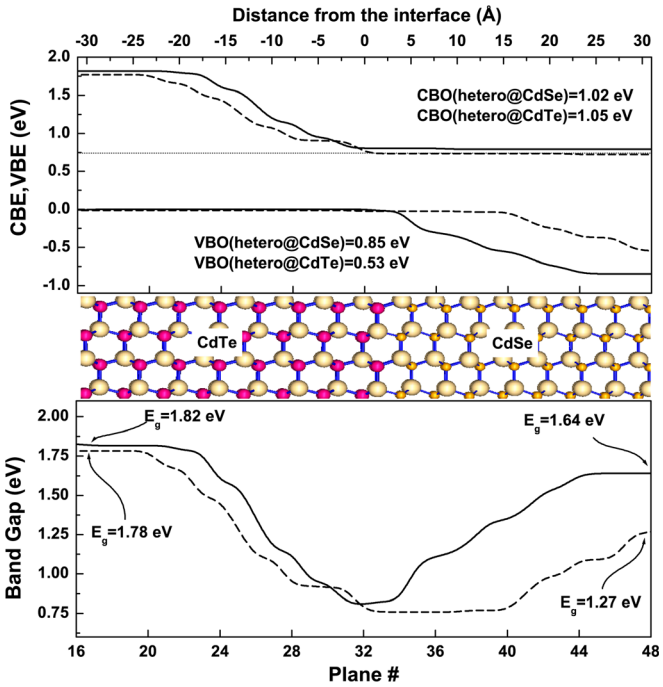

FIG. 5. Top: LDA-1/2 conduction and valence band edges along the heterojunction, from CdTe (left) to CdSe (right). Valence and conduction band offsets (VBO and CBO) indicated. Mean inter-planar distances ≈1.92 Å and ≈1.89 Å for hetero@CdSe and hetero@CdTe, respectively. Top axis show the scale, in Å, of approximate distances from the physical interface (set to zero); middle: heterostructure model (light gray: Cd; gray: Se; dark gray: Te); and bottom: LDA-1/2 band gaps (E_g) along the heterojunction, from CdTe (left) to CdSe (right). Solid and dashed lines in top and bottom panels correspond to heterojunctions with hetero@CdSe and hetero@CdTe, respectively. SO effects not included.

of the CdSe/CdTe interface bandgap over the ≈61.4 Å transition region may lead to a reinterpretation of light absorption data by this system, since the heterostructure may be more efficient at absorbing low frequency radiation than anticipated. Moreover, a bandgap smaller around the interface than in the bulk regions of CdSe and CdTe implies a larger refractive index in the same region. Therefore, a coaxial CdSe/CdTe nanowire could act as an optical waveguide as well.

Table IV summarizes the band offsets of the two CdSe/CdTe heterostructure configurations considered, comparing the LDA-1/2 results. Here, we added the bulk SO calculated energies to the VBO results without extracting the strain-induced energy changes in the valence band. Our CBOs, which do not change considerably with the substrate, are bigger than the VBOs for both configurations, indicating a higher barrier for electrons than for holes.

TABLE IV. LDA-1/2 band offsets for the two heterostructure configurations: hetero@CdTe and hetero@CdSe.

	Band offsets (eV)	
	hetero@CdTe	hetero@CdSe
CBO	1.05	1.02
VBO	0.53	0.85

IV. CONCLUSIONS

We have calculated the wurtzite CdSe and CdTe bulk electronic band gaps and their interface band offsets using the spin-unpolarized self-energy DFT/LDA-1/2 technique. The bulk bandgap energies, including SO effects, are in good agreement with experiments. For the two heterostructure cases considered, namely, strained CdSe over relaxed CdTe and vice-versa, we found that the conduction and valence band offsets extended over a ≈61 Å long region about the interface, with the conduction band transition occurring mostly in the CdTe side of the interface and the valence band transition occurring mostly in the CdSe side of the interface. As a result, the bandgap transition is not monotonic, reaching a minimum near the interface before converging to its bulk values at each side of the interface. The bandgap ranges between 0.8-1.9 eV along the transition region. This behavior may have important consequences for the interpretation of light absorption at the interface between these two materials in photovoltaic applications. Finally, we found that spin-orbit coupling energies are significant for the bulk band gaps of the two materials, but do not affect the band offsets considerably.

ACKNOWLEDGMENTS

M.R.J. thanks L. G. Ferreira, M. Marques, and L. K. Teles for fruitful discussions and guidance with the LDA-1/2 method. M.R.J. and L.R.C.F. thank D. Thober and Semp-Toshiba for financial support. The computational resources were provided by the Instituto Tecnológico de Aeronáutica under FAPESP grant 2006/05858-0 and by the Laboratory of Advanced Scientific Computation of the University of São Paulo. R.R. would like to thank the National Science Foundation for a grant partially supporting this project.

[1]M. S. Hybertsen, Mater. Sci. Eng., B **14**, 254 (1992).
[2]L. G. Ferreira, M. Marques, and L. K. Teles, Phys. Rev. B **78**, 125116 (2008).
[3]A. Alkauskas, P. Broqvist, F. Devynck, and A. Pasquarello, Phys. Rev. Lett. **101**, 106802 (2008).
[4]M. S. Hybertsen and S. G. Louie, Phys. Rev. B. **30**, 5777 (1984).
[5]M. Ribeiro, Jr., L. R. C. Fonseca, and L. G. Ferreira, Phys. Rev. B **79**, 241312 (2009).
[6]M. Ribeiro, Jr., L. Fonseca, and L. G. Ferreira, EPL. **94**, 27001 (2011).
[7]*Thin Film Solar Cells*, edited by J. Poortmans and V. Arkhipov (Wiley, 2006).
[8]H. Lee, S. W. Yoon, J. P. Ahn, Y. D. Suh, J. S. Lee, H. Lim, and D. Kim, Sol. Energy Mater. Sol. Cells **93**, 779 (2009).
[9]T. Sadowski and R. Ramprasad, J. Phys. Chem. C **114**, 1773 (2010).
[10]J. P. Perdew and A. Zunger, Phys. Rev. B **23**, 5048 (1981).
[11]G. Kresse and D. Joubert, Phys. Rev. B **59**, 1758 (1999).
[12]J. Hafner, J. Comput. Chem. **29**, 2044 (2008).
[13]H. J. Monkhorst and J. D. Pack, Phys. Rev. B **13**, 5188 (1976).
[14]S. Yang, D. Prendergast, and J. B. Neaton, Nano Lett. **10**, 3156 (2010).
[15]J. Matthews and A. Blakeslee, J. Cryst. Growth **27**, 118 (1974).
[16]X. Zhang, S. Wang, D. Ding, X. Liu, J.-H. Tan, J. Furdyna, Y.-H. Zhang, and D. Smith, J. Electron. Mater. **38**, 1558 (2009).
[17]*Semiconductors: Data Handbook*, edited by O. Madelung (Springer, 2004).
[18]J. C. Slater, Adv. Quantum Chem. **6**, 1 (1972).
[19]J. C. Slater and K. H. Johnson, Phys. Rev. B **5**, 844 (1972).
[20]O. Zakharov, A. Rubio, X. Blase, M. L. Cohen, and S. G. Louie, Phys. Rev. B **50**, 10780 (1994).
[21]*Numerical Data and Functional Relationships in Science and Technology*, Landolt- Börnstein, New Series, edited by O. M. K. H. Hellwege (Springer, 1982), Group III, Vol. 17, part A and Vol. 22, part A.

[22]H. C. Poon, Z. C. Feng, Y. P. Feng, and M. F. Li, J. Phys.: Condens. Matter **7**, 2783 (1995).
[23]S. Bloom and T. K. Bergstresser, Solid State Commun. **6**, 465 (1968).
[24]A. Kobayashi, O. F. Sankey, S. M. Volz, and J. D. Dow, Phys. Rev. B **28**, 935 (1983).
[25]D. J. Stukel, R. N. Euwema, T. C. Collins, F. Herman, and R. L. Kortum, Phys. Rev. **179**, 740 (1969).
[26]T. K. Bergstresser and M. L. Cohen, Phys. Rev. **164**, 1069 (1967).
[27]X. Chen, X. Hua, J. Hu, J.-M. Langlois, and W. A. Goddard, Phys. Rev. B **53**, 1377 (1996).
[28]Y. D. Kim, M. V. Klein, S. F. Ren, Y. C. Chang, H. Luo, N. Samarth, and J. K. Furdyna, Phys. Rev. B **49**, 7262 (1994).
[29]O. Portillo-Moreno *et al*., Opt. Mater. **18**, 383 (2002).
[30]S. G. Louie and M. L. Cohen, Phys. Rev. Lett. **35**, 866 (1975).
[31]J. M. Bass, M. Oloumi, and C. C. Matthai,. J. Phys.: Condens. Matter **1**, 10625 (1989).